Biol Trace Elem Res (2014) 162:18–25
DOI 10.1007/s12011-014-0148-8

Effects of Sodium Fluoride Treatment In Vitro on Cell Proliferation, BMP-2 and BMP-3 Expression in Human Osteosarcoma MG-63 Cells

Yan Wei · Yanli Wu · Beibei Zeng · Hua Zhang

Received: 5 August 2014 / Accepted: 2 October 2014 / Published online: 14 October 2014

Abstract Chronic excessive fluoride intake may cause fluorosis, which chiefly manifests as bone damage (or skeletal fluorosis). However, the molecular mechanism of skeletal fluorosis has not been clarified up to the present. The objective of this study was to analyze the effects of fluoride treatment on two of bone morphogenetic protein family member (BMP-2 and BMP-3) expression and cell viability using human osteosarcoma MG-63 cells as a model. Sodium fluoride (NaF) had pro-proliferation effects at relatively moderate concentration, with 5×10^3 μmol/L having the best effects. At 2×10^4 μmol/L, NaF inhibits cell proliferation. BMP-2 and BMP-3 expression was significantly induced by 5×10^3 μmol/L NaF and, to lesser extent, by 2×10^4 μmol/L NaF. Correspondingly, mothers against decapentaplegic homolog 1 (Smad-1) increased at both doses of NaF, which indicated the BMP signaling pathway was activated. Notable increases in secreted alkaline phosphatase (ALP) were observed when cells were treated with 5×10^3 μmol/L NaF. A BMP specific inhibitor LDN193189 suppressed cell proliferation induced by 5×10^3 μmol/L NaF. Also, 2×10^4 μmol/L NaF induced apoptosis but likely through a mechanism unrelated to the BMP pathway. Collectively, data show that NaF had dose-dependent effects on cell proliferation as well as BMP-2 and BMP-3 expression in MG-63 cells and suggested that cell proliferation enhanced by NaF-induced BMP members may be a molecular mechanism underlying skeletal fluorosis.

Biographical Sketch Yan Wei, Associate Professor of Guiyang Medical University.

Y. Wei · Y. Wu · B. Zeng · H. Zhang (✉)
Department of Environmental Hygiene, School of Public Health, Guiyang Medical University, 9 Beijing Road, Yunyan District, 550004 Guiyang, People's Republic of China
e-mail: schumman_wei@sina.com

Keywords Fluoride · Proliferation · Bone morphogenetic proteins · Human osteosarcoma MG-63 cells

Introduction

The halogen family element fluorine (F) is the most electronegative and reactive of all the elements. Fluorine is also a common element in the earth's crust. Elemental fluorine does not exist in nature due to its extreme reactivity, therefore always forms inorganic and organic compounds called fluorides, which represent about 0.06–0.09 % of the earth's crust's weight in the form of constituents of soil, rocks, and water [1]. For humans, fluorine is an essential trace element, preventing tooth caries at low doses [2]. Chronic excessive fluoride intake often leads to fluorosis, a toxicity which manifests as dental mottling and bone damage [3–6]. Fluorosis is recognized to be a serious global disease, occurring on all continents and affecting millions of people [7]. In China, the prevalence of endemic fluorosis affects more than 100 million people, and 2.9 million people are estimated to suffer from skeletal fluorosis [8], the most common and severe manifestation of fluoride toxicity which features osteosclerosis, ligament calcifications, and often osteoporosis, osteomalacia, or osteopenia [9, 10]. The molecular mechanism of skeletal fluorosis has not been clarified until now.

Bone morphogenetic proteins (BMPs) are members of the transformation growth factor beta (TGF-beta) superfamily of secreted signaling molecules involved in many biological processes, such as cell proliferation, differentiation, and apoptosis [11]. BMP molecules can induce ectopic cartilage and bone formation, a process that mimics embryonic endochondral bone genesis [12, 13]. Extensive studies suggest that BMPs are important in the regulation of chondrogenesis and skeletogenesis during normal embryonic development [14, 15].

BMPs constitute a family of more than 20 members, including BMP-2 and BMP-3. Previously, we found that both BMP-2 and BMP-3 were increased in the serum of rats with fluorosis [16]. These observations, although suggestive, do not rule out whether these increases in BMPs are directly related to excessive fluoride uptake [16]. Here, we investigated the relationship between NaF and BMP-2 and BMP-3 expression using a human osteosarcoma cell line, MG-63, as a model. Data indicate that NaF has dose-dependent effects on BMP expression and cell proliferation. At relatively moderate doses, NaF promotes cell proliferation and BMP expression, but at higher doses inhibits cell proliferation and less potently induces BMP expression. A BMP-specific inhibitor can suppress cell proliferation induced by NaF, suggesting that increased BMPs may be responsible for this proliferative. High doses of NaF can induce cell apoptosis, but this may be independent of the BMP pathway.

Materials and Methods

Materials

Human osteosarcoma MG-63 cells were purchased from American Type Culture Collection (ATCC; USA). Sodium fluoride (NaF, purity ≥99.99 %, CAS No. 7681-49-4, Product No. S1504) and deoxyribonucleic I (DNase I, Product No. D5025) were obtained from Sigma Chemical Company (USA). Culture medium α-MEM and trypsin were purchased from Gibco (USA). Fetal calf serum (FCS) was from Hangzhou Sijiqing Co. Ltd. (China). TRIzol was obtained from Invitrogen (USA). RevertAid™ H Minus First Strand cDNA Synthesis Kit (Product No. k1632), RiboLock™ Ribonuclease Inhibitor (Product No. EO 0381) were purchased from Fermentas (Canada) and SYBR GreenPCR Master Mix (Product No. 4472908) was from Applied Biosystems (USA). An alkaline phosphatase activity colorimetric assay kit (Product No. K412-500) was from BioVision Inc. (USA). Rabbit anti-BMP-2 polyclonal antibody, rabbit anti-BMP-3 polyclonal antibody, and mouse anti-glyceraldehyde 3-phosphate dehydrogenase (GAPDH) antibody was obtained from Proteintech™ Group Inc. (USA), Abcam PLC (UK), and Santa Cruz Biotechnology Inc. (USA), respectively. Rabbit anti-p-Smad1 was purchased from Abcam. The BMP pathway inhibitor LDN193189 was from Selleckchem, USA (CAS 1062368-24-4).

Cell Culture

MG-63 cells were cultured in α-MEM medium, supplemented with 10 % FBS, 20 mM HEPES, penicillin (100 U/mL), streptomycin (100 μg/mL), and 50 μg/mL ascorbic acid. Cells were grown at 37 °C in a humidity field atmosphere of 5 % CO_2/95 % air and were detached using 0.25 % trypsin/0.01 % EDTA.

MTT Assay

MG-63 cells were subcultured in 96-multi-well microtiter plates (1×10^4cells/mL). After overnight incubation, they were treated with 0, 10^{-2}, 10^{-1}, 1, 10, 10^2, 5×10^2, 10^3, 5×10^3, 10^4, 2×10^4, and 4×10^4 μmol/L NaF for 48 h. MTT dye at a final concentration of 5 mg/L was added to each well. Cells were incubated with MTT at 37 °C for 4 h, then media was carefully removed, and 150 μL DMSO was added to the cells to stop the reaction. Finally, the optical density in each well was measured with an ELISA reader at a wavelength of 590 nm. The effect of each NaF concentration on cell viability was evaluated using averages of three wells, and untreated MG-63 cells were considered 100 % viable. MTT assay revealed that 10^2, 5×10^3, and 2×10^4 μmol/L were suitable doses for subsequent experiments.

Alkaline Phosphatase Activity Colorimetric Assay

Alkaline Phosphatase (ALP) quantification was performed with an ALP assay kit according to the manufacturer's instructions (No. K412-500, BioVision, USA).

Cell Cycle Analysis

The effects of NaF on cell cycle analysis were assessed by flow cytometry using propidium iodide. Briefly, MG-63 cells were plated in 6-well plates overnight and then treated with 0, 10^2, 5×10^3, 2×10^4 μmol/L NaF for 48 h. Cells were harvested using trypsin/EDTA and washed twice in cold phosphate-buffered saline (PBS) containing 0.1 % BSA. After fixing with 70 % ethanol at 4 °C overnight, cells were incubated with 100 μL propidium iodide and 100 μL RNase A (10 mg/mL) at 37 °C in the dark for 30 min. The percentage of cells in different cell cycle phases were measured with a FACSort Flow Cytometer at 488 nm, and data were analyzed with ModFit software. A proliferation index (PI) was calculated with the following equation: PI=(S+G2/M)/(S+G2/M+G0/G1). The effects of each treatment on the cell cycle were measured in a minimum of three replicates.

Cell Apoptosis

Cell apoptosis was measured using the Annexin V-FITC & PI Apoptosis Detection Kit (ADL, A0001a) according to the manufacturer's instructions. Briefly, 10^5–10^6 cells were labeled with 5 μL Annexin V-FITC in a 100 μL reaction

system. Apoptosis of the MG-63 cells (%) was analyzed by flow cytometry using a BD FACSAria flow cytometer.

qRT-PCR Analysis for BMP-2 and BMP-3 mRNA

MG-63 cells were plated in 6-wells plates, and after overnight incubation at 37 °C, cells were treated with 0, 10^2, 5×10^3, and 2×10^4 μmol/L NaF for 48 h. Total RNA of treated cells was extracted using TRIzol regent. Briefly, 0.8 mL TRIzol was added into each well and incubated at room temperature for 10 min. Lysate was transferred into a 1.5 mL EP tube and 0.2 mL chloroform was added. The mixture was shaken vigorously and centrifuged at 12,000×*g* at 4 °C for 15 min. Upper aqueous phase was transferred into another clean tube. RNA was precipitated from the aqueous phase by mixing with 0.5 mL isopropyl alcohol. Samples were incubated at room temperature for 10 min and centrifuged at 12,000×*g* at 4 °C for 15 min. Supernatant was removed, and RNA pellets were washed once with 1 mL 75 % ethanol. After air-drying for 10 min, RNA was dissolved in RNase-free water. Genomic DNA was removed from the sample by DNase treatment (1 U/μL DNase I in DNase I buffer at 37 °C for 30 min). RNA concentration and purity were measured by spectrophotometry and an OD_{260}/OD_{280} ratio exceeding 1.8 was considered acceptable. RNA quality was confirmed by electrophoresis on a 1 % agarose gel followed by visual confirmation of ribosomal RNA (28, 18, and 5S).

First-strand cDNA was synthesized using RevertAid™ H Minus First Strand cDNA Synthesis Kit. Relative quantification of BMP-2 and BMP-3 gene transcripts was carried out by fluorescence-based real-time quantitative PCR on an ABI PRISM 7900 sequence detection system (Applied Biosystems, USA) using SYBR GreenPCR Master Mix. Primers (Table 1) for quantitative PCR (qPCR) were designed based on available human sequences in GenBank for BMP-2, BMP-3, and GAPDH using Primer Premier 5.0 software. Primer specificity was first tested by conventional reverse transcription polymerase chain reaction (RT-PCR). The human housekeeping gene GAPDH was used as an internal control. PCR reaction conditions were as follows: 94 °C (20 s), 59 °C (20 s), and 72 °C (20 s) for 40 cycles. All qPCR analyses were repeated at least three times.

Western Blot Analysis

MG-63 cells were plated in 6-well plates, and after overnight incubation at 37 °C, cells were treated with 0, 10^2, 5×10^3, and 2×10^4 μmol/L NaF for 48 h. Cells were lysed with Triton lysis buffer (50 mM Tris-HCl pH 8.0, 150 mM NaCL, 1 % Triton X-100, 0.02 % sodium azide, 10 mM EDTA, 10 μg/mL aprotinin, and 1 μg/mL aminoethylbenzene sulfonyl fluoride). Protein concentrations were measured using the Bradford assay. Then, 100 μg proteins from each well was loaded onto a 10 % polyacrylamide gel. After electrophoresis, SDS-PAGE-separated proteins were transferred to a PVDF membrane. Then, the membrane was blocked with 5 % skim milk for 1 h followed by a PBS containing 0.1 % Tween (PBST) wash. The membrane was incubated with anti-BMP-2, anti-BMP-3, and anti-GAPDH antibody at 1:400, 1:400, and 1:800 dilutions, respectively, for 2 h at room temperature. After washing with PBST, the membrane was incubated with 1:10,000 diluted HRP-conjugated secondary antibodies for 1 h at room temperature. Immunoreactive bands were visualized using luminal reagents and Hyper ECL film (Amersham Biosciences) according to the manufacturer's instructions. The integrated optical density (IOD) of each band was measured with Gel-Pro Analyzer 4.0 software (Media Cybernetics, USA).

Statistical Analysis

Results are expressed as means ± standard deviation. One-way analysis variance (ANOVA) was used to analyze differences among various groups. Further multiple comparisons were analyzed using the Student-Newman-Keuls (SNK) method. *P* values less than 0.05 were judged to be statistically significant.

Results

Dose-Dependent Effects of NaF Treatment on MG-63 Cell Viability

The effects of various concentrations of NaF and treatment intervals on MG-63 cell viability were analyzed by MTT

Table 1 Primer sequences with corresponding PCR size and accession

Primer	Sequence (5′→3′)	Product (bp)	GenBank accession no.
BMP-2-F	ACTCGAAATTCCCCGTGACC	144	NM001200
BMP-2-R	CCACTTCCACCACGAATCCA		
BMP-3-F	TCCTGGGGCAGAATACCAGT	148	NM_001201.1
BMP-3-R	AAATTGGAGCGTCTGGCTCT		
GAPDH-F	CAATGACCCCTTCATTGACC	106	NM_002046.4
GAPDH-F	GACAAGCTTCCCGTTCTCAG		

assay, which was shown in Fig. 1. Treatments at 24, 48, and 72 h NaF treatment had similar trends, with 48 h promoting the greatest cell viability. So, NaF treatment at 48 h was used in subsequent experiments. At very low doses, NaF had negligible effects on cell viability, but cell viability increased up to 10^2 μmol/L NaF. Positive NaF effects on cell viability peaked at 5×10^3 μmol/L NaF and further increases in NaF diminished promotion of cell viability. At 2×10^4 μmol/L NaF, cell viability was inhibited. Thus, 10^2, 5×10^3, and 2×10^4 μmol/L (low, medium, and high-dose NaF) were studied in subsequent experiments.

Dose-Dependent Effects of NaF on Cell Cycle Phases of MG-63 Cells

MTT assay measures not only proliferating cells but also metabolically active cells. To confirm that NaF affects cell proliferation, flow cytometry was used to measure the effects of NaF on the cell cycle. Cell cycle data by flow cytometry is depicted in Fig. 2. MG-63 cell treatment with 10^2 μmol/L NaF for 48 h did not change the PI or the cell cycle phases compared to control. Among the three tested concentrations, 5×10^3 μmol/L NaF caused the highest PI and the greatest number of cells in the G2M and S phases as well as the fewest cells in G0G1 and subG0 phases, demonstrating a pro-proliferation effect. In contrast, 2×10^4 μmol/L NaF had the lowest PI and the fewest cells in the G2M and S phases and the most cells in the G0G1 and subG0 phases, indicating an anti-proliferation effect. These data indicate that NaF has dose-dependent effects on cell proliferation.

High-Dose NaF Induces Apoptosis in MG-63 Cells

Since high-dose NaF can suppress cell proliferation and decrease viable cells, it may induce apoptosis. Cell apoptosis induced by three NaF concentrations were measured with flow cytometry using an Annexin V-FITC method. Figure 3a is the representative data analyzed by flow cytometry, and the lower right quadrant showed the apoptosis cells; high-dose NaF induced the highest percentage of apoptosis cells (Fig. 3b). We can also get the information of necrotic cells corresponding to the upper right quadrant by this method. The one which had the most percentage of necrotic cells was 2×10^4 μmol/L NaF also.

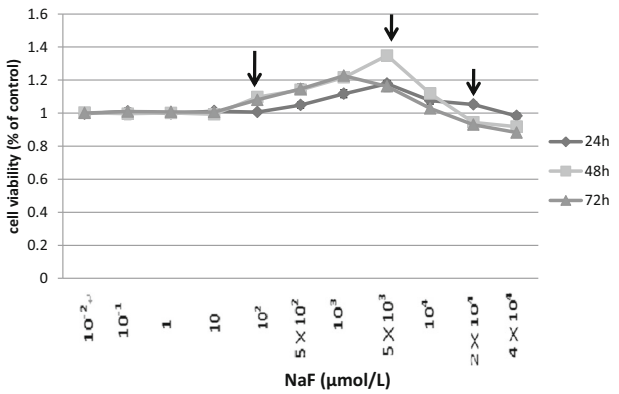

Fig. 1 Effects of NaF on relative viability of MG-63 cells measured by MTT assay. Cells were treated with 0, 10^{-2}, 10^{-1}, 1, 10, 10^2, 5×10^2, 10^3, 5×10^3, 10^4, 2×10^4, or 4×10^4 μmol/L NaF for 24, 48, or 72 h, respectively. Viability of untreated cells was defined as 100 %

Dose-Dependent Effects of NaF on BMP-2 and BMP-3 Expression

After documenting dose-dependent effects of NaF on proliferation and apoptosis in MG-63 cells, we investigated the underlying molecular mechanism. Because BMP-2 and BMP-3 were increased in serum of rats with fluorosis and there is a critical role of BMP in osteogenesis, NaF's effect on BMP-2 and BMP-3 was investigated. Relative messenger RNA (mRNA) of BMP-2 and BMP-3 was measured by qRT-PCR (See Fig. 4a, b). Cells treated with 5×10^3 μmol/L NaF had the highest BMP-2 and BMP-3 mRNA among all groups ($P<0.05$). Also, 2×10^4 μmol/L NaF was less effective for inducing BMP-2 and BMP-3 mRNA than 5×10^3 μmol/L NaF, but still better than 10^2 μmol/L NaF and the empty control.

To determine whether changes in mRNA changed protein, we measured relative protein of BMP-2 and BMP-3 by Western blot. As shown in Fig. 4c, d, in agreement with mRNA results, 5×10^3 μmol/L was the most potent concentration of NaF for inducing BMP-2 and BMP-3 proteins, and 2×10^4 μmol/L NaF was less potent but still better than 10^2 μmol/L NaF and the empty control (see Fig. 4e).

Thus, our data indicate that dose-dependent effects of NaF on BMP-2/3 expression correlate well with its effects on cell proliferation, suggesting that BMP-2/3 and the BMP signaling pathway may be, at least, a molecular mechanism behind this event.

Elevated BMPs Activate BMP Signaling Pathway to Promote Cell Proliferation

To test whether increased BMP-2/3 can activate the BMP signaling pathway in MG-63 cells, we measured phosphorylation of mothers against decapentaplegic homolog 1 (p-Smad1), a common indicator of BMP pathway activation. Indeed, p-Smad1 was significantly increased by 5×10^3 or 2×10^4 μmol/L NaF, indicating that the BMP pathway was activated by these two doses (Fig. 5a). Also, 10^2 μmol/L NaF had little effect on p-Smad1, and this was consistent with its modest effect on BMP-2/3 expression.

Dose-dependent activation of the BMP pathway by NaF correlates well with its dose-dependent effects on cell

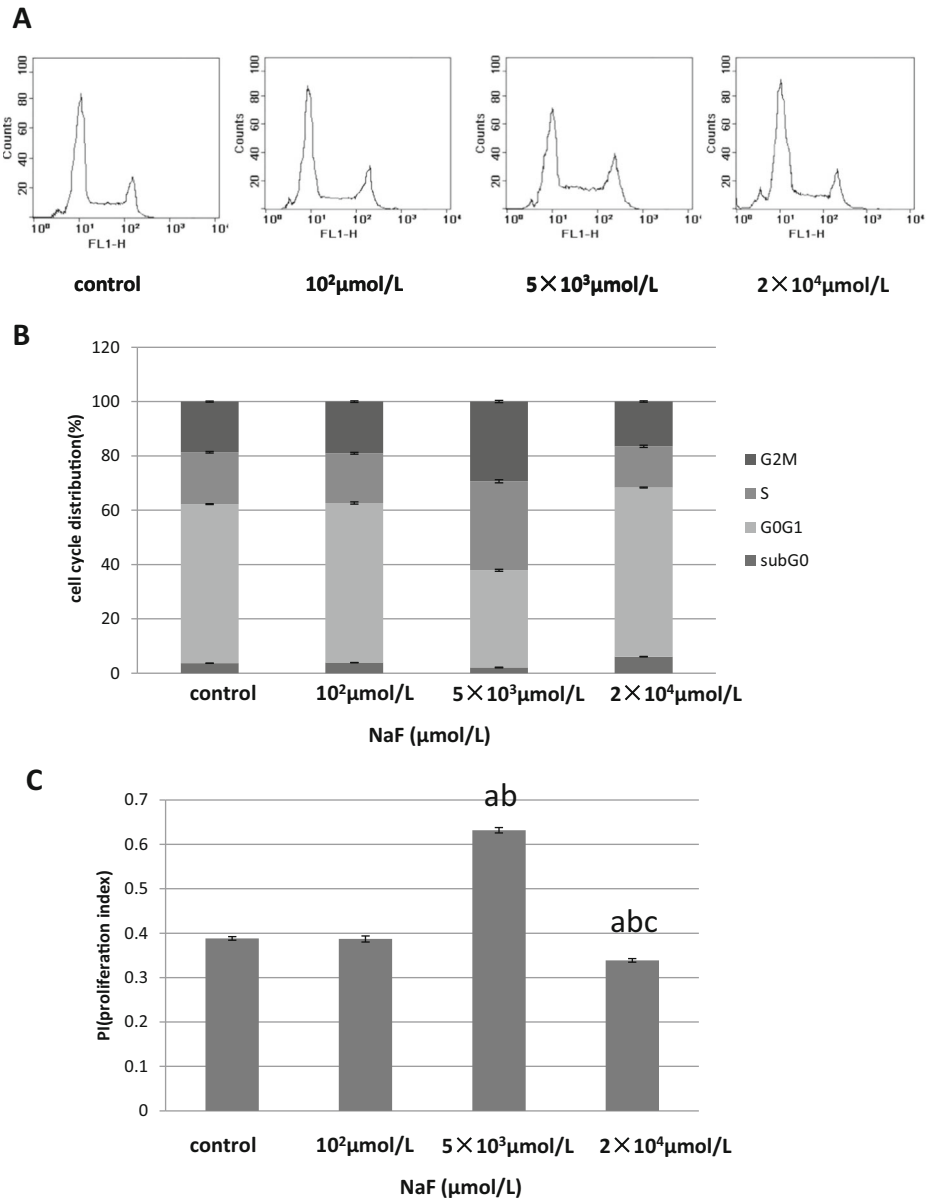

Fig. 2 Effects of NaF treatment on cell cycle of MG-63 cells. **a**. Representative flow cytometry data of cells treated with various concentrations of NaF. **b**. Quantitative results of cell cycle analysis by flow cytometry. The percentage of cells in the subG0, G0/G1, S, G2/M phases of the cell cycle were estimated using ModFit software. The relative distribution of the cell population in a specific phase of the cell cycle was altered in the group treated with 5×10^3 and 2×10^4 μmol/L NaF. **c**. Comparison of proliferation indices (PI) of different groups PI=(S+G2/M)/(S+G2/M+G0/G1). The data plotted as *bars* are means ± standard error (SE) of three replicates (three parallel measurements in the single experiment). The letter *a* indicates $P<0.05$ vs. control, *b* is $P<0.05$ vs. cells treated with 10^2 μmol/L NaF, and *c* is $P<0.05$ vs. cells treated with 5×10^3 μmol/L NaF

proliferation, suggesting a model wherein NaF induces BMP-2/3 expression to activate the BMP pathway, promoting cell proliferation. To confirm this model, a BMP specific inhibitor, LDN193189, which can completely suppress Smad1 phosphorylation induced by BMP-4 at ~40 nmol/L [17], was used to block BMP pathway activation. We observed that 40 nM LDN193189 suppressed cell proliferation induced by 5×10^3 μmol/L NaF, supporting a BMP pathway-mediated model of NaF-induced cell proliferation (Fig. 5b).

Because activation of the BMP pathway induces bone and cartilage formation [12, 13], we investigated whether NaF could induce expression of ALP which plays an important role in the mineralization of bone. Notable increases in secreted ALP were observed when cells were treated with 5×10^3 μmol/L NaF for 48 h (Fig. 5c).

Discussions

The MTT assay is a classical approach for assessing cell viability, so this was used to measure effects of NaF on MG-63 cell viability. Data indicate a dual effect of NaF on MG-63 cell viability: low concentrations of NaF promoted MG-63 cell viability and higher concentrations reduced cell viability. To confirm that NaF affected cell proliferation in a dose-dependent manner, the cell cycle was analyzed by flow cytometry. The results were corresponding with that of MTT assay, which indicated that low concentrations of NaF (5×10^3 μmol/L) promote cell proliferation, and high concentration (2×10^4 μmol/L) reduces MG-63 cell proliferation. Previous work indicates that treatment with 10^{-5} mol/L NaF increased proliferation and ALP activity of primary bone cells

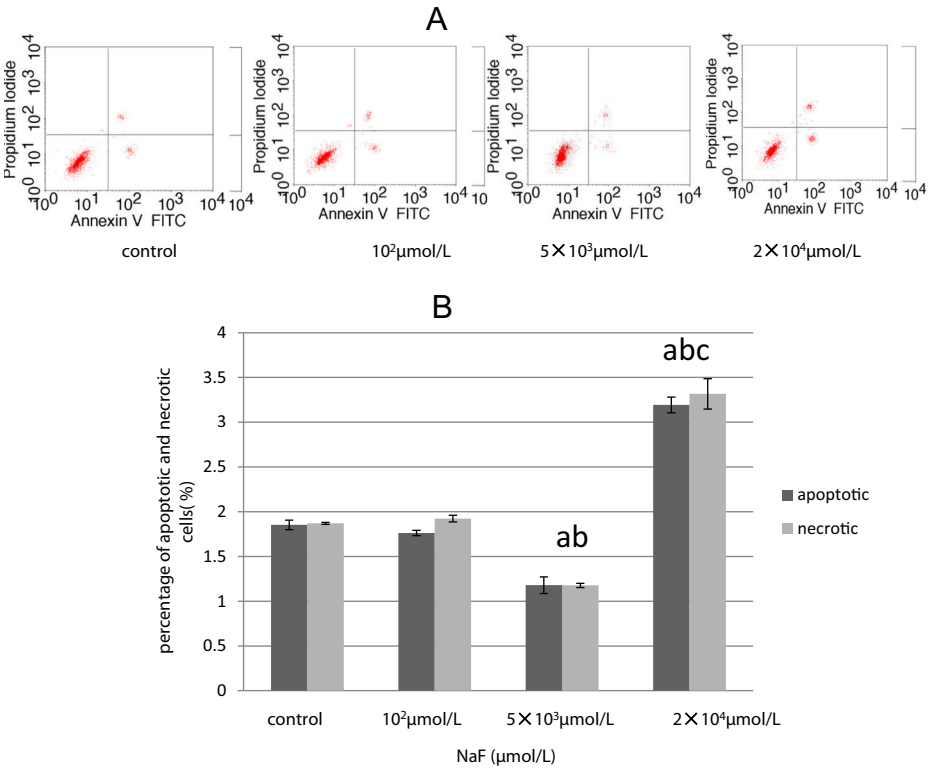

Fig. 3 Effects of NaF on MG-63 cell apoptosis. **a**. Representative cell apoptosis data analyzed by flow cytometry using an Annexin V-FITC method. **b**. Quantitative cell apoptosis and necrosis data (plotted as *bars* are means±SE of three parallel measurements in the single experiments). The letter *a* indicates $P<0.05$ vs. control, and *b* is $P<0.05$ vs. cells treated with 10^2 μmol/L NaF)

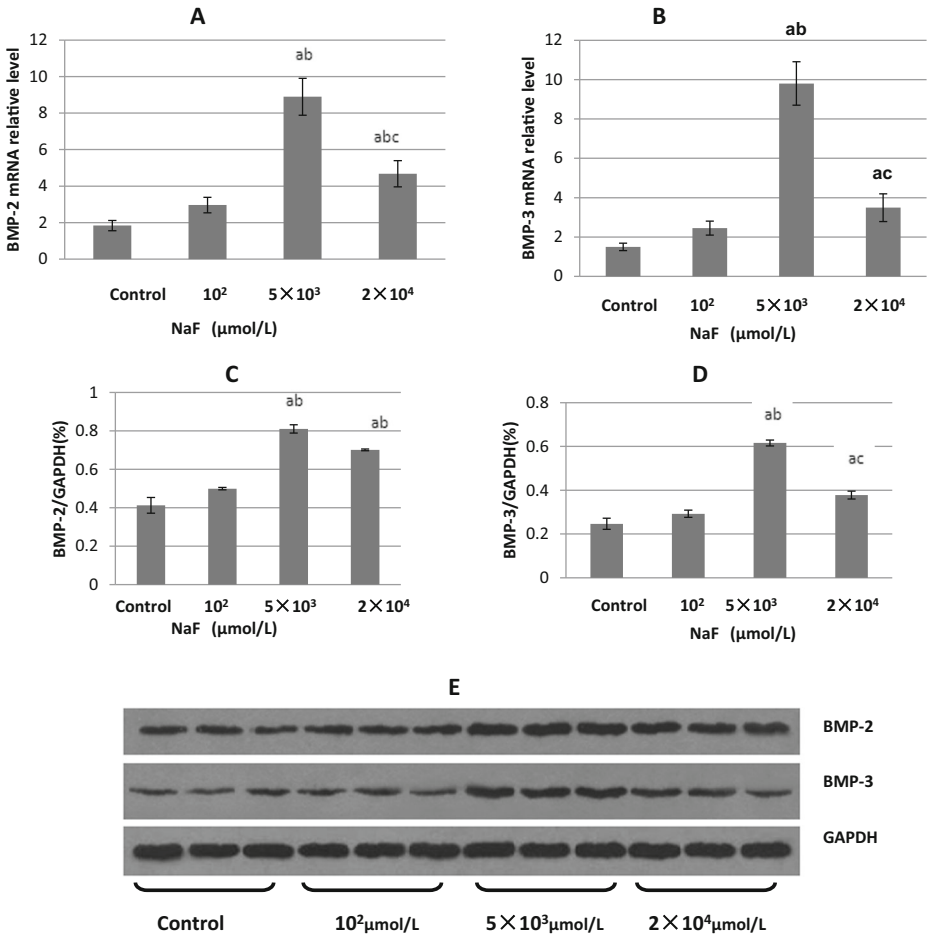

Fig. 4 Effect of NaF treatment on BMP-2 and BMP-3 expression. **a**. Relative BMP-2 mRNA. **b**. Relative BMP-2 mRNA (data plotted as *bars* are means±SE of three parallel measurements in the single experiment. The letter *a* indicates $P<0.05$ vs. control, *b* is $P<0.05$ vs. cells treated with 10^2 μmol/L NaF, and *c* is $P<0.05$ vs. cells treated with 5×10^3 μmol/L NaF) **c**. Density quantization of BMP-2 protein expression. **d**. Density quantification of BMP-3 protein expression (data plotted as *bars* are means±SE of three parallel measurements in the single experiments. The letter *a* indicates $P<0.05$ vs. control, *b* is $P<0.05$ vs. cells treated with 10^2 μmol/L NaF, and *c* is $P<0.05$ vs. cells treated with 5×10^3 μmol/L NaF.) **e**. Western blot analysis of BMP-2, BMP-3, and GAPDH protein expression in MG-63 cells treated with various concentrations of NaF

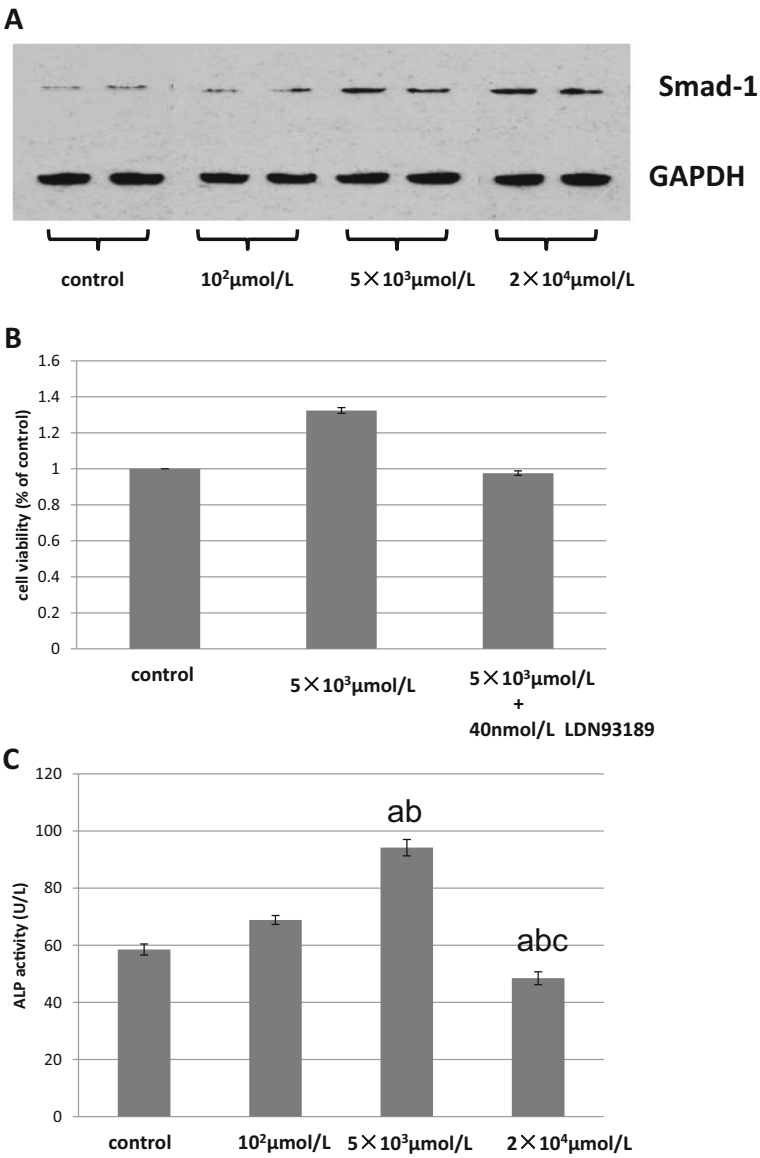

Fig. 5 NaF activates BMP signaling pathway to stimulate cell proliferation and mineralization. **a**. Cells treated with 5×10^3 or 2×10^4 μmol/L NaF increased Smad1 phosphorylation. **b**. Cell proliferation induced by NaF was suppressed by the BMP pathway specific inhibitor LDN193189. Cell viability was measured by MTT assay, and viability of control cells was defined as 100 %. **c**. Cells treated with 5×10^3 μmol/L NaF show increased ALP activity (data plotted as *bars* are means±SE of three parallel measurements in the single experiments. The letter *a* indicates $P<0.05$ vs. control, *b* is $P<0.05$ vs. cells treated with 10^2 μmol/L NaF, and *c* is $P<0.05$ vs. cells treated with 5×10^3 μmol/L NaF)

in vitro [18]. However, NaF greater than 10^{-4} mol/L inhibited proliferation and increased apoptosis of primary osteoblast in vitro [19, 20]. In rat osteosarcoma UMR-106 cells, 10^{-6} mol/L NaF promoted both proliferation and ALP activity, while 10^{-4} mol/L NaF suppressed both [21]. Testing murine osteoblasts such as MC3T3-E1 cells with the MTT assay revealed that NaF did not enhance cell viability. These data agree with the previous work [22]. Collectively, the effect of NaF on cell proliferation is concentration and cell type dependent.

Although the dose-dependent effects of NaF on MG-63 cell proliferation are evident, the underlying molecular mechanism is unclear. Previously, we found that two BMP actors, BMP-2 and BMP-3, were increased in the serum of rats with fluorosis. BMPs are morphogens essential for skeletal development and can induce both osteoblast and chondrocyte differentiation of mesenchymal cells [23, 24]. BMPs bind to two different types of serine-threonine kinase receptors, types I and II, to activate intracellular signals mediated by Smad proteins [25]. Activated Smad1, Smad5, and likely MADH6 form heteromeric complexes with Smad4 and then translocate into the nucleus where they can activate transcription of various genes [25]. Members of the BMP family have distinct spatiotemporal expression patterns, and their biological activities are not identical. BMP-2 and BMP-3 both strongly induce bone formation [25]. In light of the critical role of BMPs in bone formation and elevated BMP-2/3 in sera of rats with fluorosis, possibly, NaF induces expression of BMP-2 and BMP-3 to promote cell proliferation, and we provided evidence to support this model. First, we showed that NaF can induce expression of BMP-2 and BMP-3 in a dose-dependent manner. Next, 5×10^3 μmol/L NaF was the best concentration

for inducing BMP-2 and BMP-3 expression, and 2×10^4 μmol/L NaF, albeit less effective than 5×10^3 μmol/L NaF, could induce BMP-2 and BMP-3 expression. Second, increased BMP-2/3 led to activation of the BMP pathway, as indicated by elevated phosphorylation of Smad1. Finally, the BMP pathway inhibitor LDN193189 abolished NaF-induced cell proliferation, confirming this model.

NaF has been reported to enhance BMP protein activity when it was mixed with BMP and implanted under the abdominal skin of Wistar rats [26]. Thus NaF may activate the BMP pathway through dual mechanisms, i.e., on one hand, it increases BMP expression and, on the other hand, it enhances BMP activity. Still, this model cannot explain cell apoptosis induced by high concentrations of NaF. Although 2×10^4 μmol/L NaF can induce BMP expression, it triggered apoptosis. High-dose NaF can activate other signaling pathways to elicit apoptosis [1]; therefore, the mechanism underlying NaF-induced apoptosis may not be related to the BMP pathway.

In summary, NaF regulates BMP-2/3 expression in a dose-dependent manner to affect cell proliferation at relatively low concentrations. High NaF concentrations, although still able to induce BMPs, may activate other signaling pathways to stimulate apoptosis. NaF induction of BMPs to activate the BMP signaling pathway to stimulate cell proliferation may be a molecular mechanism underlying skeletal fluorosis.

Acknowledgments This study was supported by the National Natural Science Foundation of China (81360412) and Science and Technology Funds from the Department of Science and Technology of Guizhou Province (No. SY [2013] 3062 and J [2010] 2268).

Conflict of Interest No conflict of interest exits in the submission of this manuscript, and manuscript is approved by all authors for publication. The work described was original research that has not been published previously and not under consideration for publication elsewhere. The opinions expressed by the authors contributing to this journal do not necessarily reflect the opinions of the Guiyang Medical University with which the authors are affiliated.

References

1. Agalakova NI, Gusev GP (2012) Molecular mechanisms of cytotoxicity and apoptosis induced by inorganic fluoride. ISRN Cell Biology 2012:1–16
2. Heller KE, Eklund SA, Burt BA (1997) Dental caries and dental fluorosis at varying water fluoride concentrations. J Public Health Dent 57:136–43
3. Chachra D, Turner CH, Dunipace AJ et al (1999) The effect of fluoride treatment on bone mineral in rabbits. Calcif Tissue Int 64: 345–51
4. Fejerskov O, Manji F, Baelum V (1990) The nature and mechanisms of dental fluorosis in man. J Dent Res 69:692–700
5. Grynpas MD (1990) Fluoride effects on bone crystals. J Bone Miner Res 5:169–75
6. Mousny M, Omelon S, Wise L et al (2008) Fluoride effects on bone formation and mineralization are influenced by genetics. Bone 43: 1067–1074
7. Organization WH (2006) Country data on dental and skeletal fluorosis associated with exposure to fluoride through drinking-water. In: Fawell J (ed) Fluoride in drinking-water. IWA Publishing, London, pp 97–125
8. Sun D, Sun Y (2005) Report on epidemiology investigation of endemic fluorosis in China. Chin J Epidemiol 20:81–84
9. Christie DP (1980) The spectrum of radiographic bone changes in children with fluorosis. Radiology 136:85–90
10. Wang W, Kong L, Zhao H et al (2007) Thoracic ossification of ligamentum flavum caused by skeletal fluorosis. Eur Spine J 16: 1119–28
11. Massague J (1998) TGF-beta signal transduction. Annu Rev Biochem 67:753–791
12. REDDI AH, HUGGINS C (1972) Biochemical sequences in the transformation of normal fibroblasts in adolescent rats. Proc Natl Acad Sci 69:1601–5
13. Reddi AH (1981) Cell biology and biochemistry of endochondral bone development. Coll Relat Res 1:209–26
14. Sandrine P, Lee N (2000) BMPs are required at two steps of limp chondrogenesis: formation of prechondrogenic condensations and their differentiation into chondrocytes. Dev Biol 219:237–49
15. Macicas D, Ganan Y, Sampath TK et al (1997) Role of BMP-2 and OP-1 (BMP-7) in programmed cell death and skeletogenesis during chick limb development. Development 124:1109–17
16. Wei Y, Zhang Z, Long JF et al (2013) Expression of bone morphogenetic protein in coal-burning fluorosis rats. Chin J Epidemiol 32: 374–377
17. Yu PB, Deng DY, Lai CS et al (2008) BMP type I receptor inhibition reduces heterotopic ossification. Nat Med 14:1363–9
18. Farley JR, Wergedal JE, Baylink DJ (1983) Fluoride directly stimulates proliferation and alkaline phosphatase activity of bone-forming cells. Science 222:330–2
19. Yan X, Feng C, Chen Q et al (2009) Effects of sodium fluoride treatment in vitro on cell proliferation, apoptosis and caspase-3 and caspase-9 mRNA expression by neonatal rat osteoblasts. Arch Toxicol 83:451–8
20. Yan X, YAN X, Morrison A et al (2011) Fluoride induces apoptosis and alters collagen I expression in rat osteoblasts. Toxicol Lett 3:133–8
21. Long L, Li L, Liu K et al (2004) Study on effect of sodium fluoride on osteoblast-like cell in vitro. China Prev Med 5:168–71
22. Cai R, Guo X, Zhao X et al (2009) Effects of fluoride and aluminum alone and combination exposure on proliferation and cell cycle of MC3T3-E1 cells. J Environ Health 26:1089–91
23. Chen D, Ji X, Harris MA et al (1998) Differential roles for bone morphogenetic protein (BMP) receptor type IB and IA in differentiation and specification of mesenchymal precursor cells to osteoblast and adipocyte lineages. J Cell Biol 142:295–305
24. Ryoo HM, Lee MH, Kim YJ (2006) Critical molecular switches involved in BMP-2-induced osteogenic differentiation of mesenchymal cells. Gene 366:51–7
25. Kawabata M, Imamura T, Miyazono K (1998) Signal transduction by bone morphogenetic proteins. Cytokine Growth Factor Rev 9:49–61
26. Xu S, Zheng G, Li M, Shu B (2000) Direct effects of fluoride on activities of bone morphogenetic protein. Zhonghua Yu Fang Yi Xue Za Zhi 34:215–7